J MATER SCI 41 (2006) 3837–3843

Characterisation of barium titanate-silver composites, part I: Microstructure and mechanical properties

S. PANTENY*, C. R. BOWEN, R. STEVENS
Materials Research Centre, Department of Engineering and Applied Science, University of Bath, Bath BA2 7AY, UK

Published online: 10 April 2006

The paper presents an investigation of the influence of silver particles on the microstructure and mechanical properties of barium titanate. Barium titanate-silver composites have been prepared by ball milling precursor powder constituents; followed by drying, sieving and calcination prior to powder compaction. After sintering the green compacts, microstructural analysis was undertaken involving measurement of grain size, silver particle size, phase composition and phase content. Characterisation of mechanical strength, toughness, hardness and stiffness was also undertaken. Reaction product phases between silver and barium titanate could not be detected. The dispersed silver particles were shown to inhibit densification. Silver particles below 1 μm in size were intragranular and attached to domains. The size of the intergranular silver particles increased with silver content. An increase in silver content improved whereas strength, hardness and stiffness decreased, while toughness was unchanged.

1. Introduction

Barium titanate and lead zirconate titanate (PZT) are well established electroceramics that have been extensively studied in the pure and doped forms. Recently, the effect of second phase additions such as alumina [1], and ductile particles, such as platinum [2] and silver [3], has been reported as a method of increasing both mechanical and dielectric properties of ceramics. Silicon carbide particles have been used to enhance the mechanical properties of structural ceramics, such as alumina [4], and also have been added to electroceramics, such as barium titanate, in an effort to enhance the relatively poor mechanical properties [5]. While improvements in strength have been observed, previous work on the barium titanate-silicon carbide system indicates that reaction products, in the form of a semi-conducting matrix, can result [6]. This suggests that although there may be benefits in terms of mechanical properties, there may also be a reduction in electrical properties.

The aim of this work is to present a detailed and systematic characterisation of a particulate reinforced piezoelectric composite. In this study ductile, high conductivity silver particles have been added to barium titanate in order to provide an understanding of the influence of these additions on mechanical and electrical properties, along with modelling of the composite system. This paper presents observations of reaction phase formation, changes in microstructure and modifications to mechanical properties. The system has been chosen due to relative ease of fabrication and that the solubility between silver and barium titanate is considered to be negligible [7].

Previous workers that have fabricated barium titanate-silver composites have used silver nitrate [3, 7–9] as the silver source and added a maximum of 10 wt.%. It has been reported that silver diffusion is limited in barium titanate [8], its presence decreases density [9, 10], grain size, silver inclusion size and toughness [3]. The solubility limits of silver in barium titanate is low and does not change the c/a ratio or Curie temperature [7] and no reaction phase has been detected [9]. Strength has been reported to increase by ~20% with 0.5 wt.% silver addition [7]. The relative permittivity appears to depend on density, grain size and silver content [3] with a decrease to a plateau <0.2 wt.% silver [7], a 10% maximum increase at ~0.3 wt.% silver [10] and 50% increase with 10 wt.% silver [9] have all been reported. Part 2 of the paper will discuss the electrical properties.

*Author to whom all correspondence should be addressed.
0022-2461
DOI: 10.1007/s10853-005-5163-x

2. Experimental procedure

Barium titanate powder (Morgan Electroceramics, 1–2 μm) and silver nitrate (Aldrich, 20913-9) were attrition milled with ethanol in a zirconia container for 2 h using 5 mm diameter zirconia media. The slurry was dried under an infra-red lamp and sieved (150 μm mesh). The powder was calcined at 300°C for 2 h to decompose the silver nitrate to metallic silver. Green compacts were formed by uni-axial die pressing at 50 MPa and were further consolidated using cold isostatic pressing at 150 MPa. The disc samples were sintered at 1300°C for 2 h using a ramp rate of 180°C/h. Composites were produced with 0, 1.3, 3.2, 6.4, 9.5, 12.7, 15.9 and 19.1% silver by weight, corresponding to volume fractions of 0, 0.7, 1.8, 3.7, 5.6, 7.6, 9.7 and 11.8 vol.%; silver loss by evaporation from the surface was ignored.

Dilatometry was undertaken using a Netzsch Dil 402C (Netzsch Tasc 414/4 controller) to examine any changes in the sintering kinetics between the monolithic and composite materials. The density of the composites was determined using the Archimedes water immersion technique. Sintered samples were ground and subjected to X-ray diffraction analysis (XRD), using CuK_α radiation, to establish that all the silver nitrate had decomposed to silver, and that no chemical reactions had occurred between the silver particles and barium titanate matrix. Samples were ground and polished to a 3 μm finish for microstructural analysis by optical and scanning electron microscopy, (JEOL JSM-T330). Chemical etching was accomplished using a solution of nitric acid and hydrofluoric acid (H_2O + 4%HNO_3 + 2%HF) for 20–60s.

Surface grinding removed an outer layer depleted in silver, to a depth of approximately 50 μm. Samples bars were polished to 1 μm finish for fracture strength, hardness and toughness measurements. Fracture strength was measured on samples with dimensions in the ranges of 1.8–2.3 mm and 11.2–12.8 mm for the thickness and diameter, respectively, using the ball-on-ring technique with a loading rate of 0.5 mm/min using an Instron 1122. Hardness and toughness evaluation used a 98 N load applied for 30 s by means of a Zwick 3212B Hardness Tester. The indent diagonals and crack lengths thus formed were measured optically, and used to calculate the Vickers hardness and the fracture toughness, respectively. The stiffness of each of the composites was determined by resonance analysis on poled samples using a Solartron 1296 Dielectric Interface and S11260 Impedance/Gain phase analyser.

3. Results and discussion

3.1. Sintering kinetics and final densities

Dilatometry of the monolithic barium titanate indicated two sintering rate peaks at 1170°C and 1300°C, Fig. 1, in agreement with the literature [11]. The first peak relates to grain boundary solid-state diffusion, while the higher temperature peak is considered to be due to liquid phase sintering [11]. The addition of silver reduced the temperature

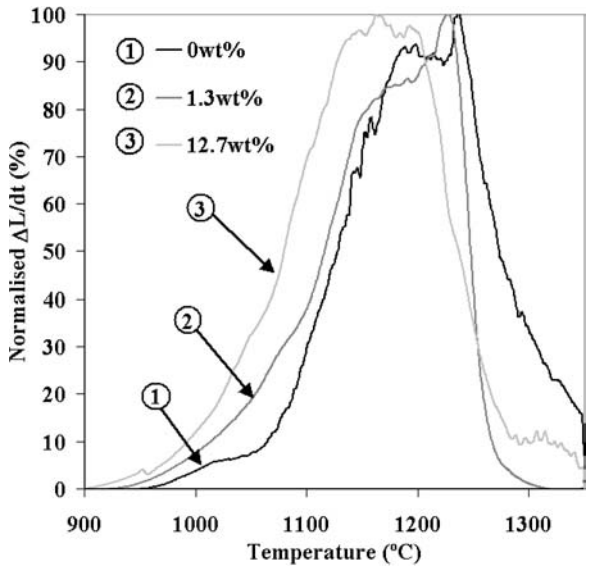

Figure 1 Dilatometry results for barium titanate with silver contents of 0, 1.3 and 12.7 wt.%.

at which sintering began and a broad high sintering rate from 1150°C to ~1220°C was observed for the barium titanate-12.7 wt.% silver composite. It has been suggested that enhanced densification of PZT with silver additions is due to a slight dissolution of silver into the ceramic matrix, which either increases the defect concentration or decreases the liquid phase formation temperature [3], although silver has a lower solubility in barium titanate [7]. The overall percent shrinkage after sintering was reduced with small silver additions (~15% shrinkage) in comparison to the monolith (17% shrinkage).

At higher silver contents (>15 wt.%) the shrinkage on sintering was similar to that of the monolith, and is suggested to be due to the silver connectivity being sufficient such that capillary pressure and surface tension aid sample contraction. Sintering of the pure barium titanate starting powder produced samples with a final density of 94.5%, a typical value [12]. Metallic silver is liquid at the sintering temperature (silver melting point is ~960°C) and reduces the final sintered density, as shown in Fig. 2, due to the molten silver reducing connectivity of barium titanate particles. Silver is readily vapourised from the specimens' surface and interior regions above its melting point. As such, the weight fraction of silver after sintering will be reduced from the starting value. After sintering barium titanate and composites were observed to be in an oxidised state as they were not black in colour, indicating dielectric properties [13].

3.2. Microstructural analysis

XRD analysis did not detect any phases other than barium titanate or silver after sintering at 1300°C (Fig. 3). Complete decomposition during sintering of the silver nitrate to silver, with a lack of reaction phases between the barium titanate and silver was confirmed. Fig. 3 shows the

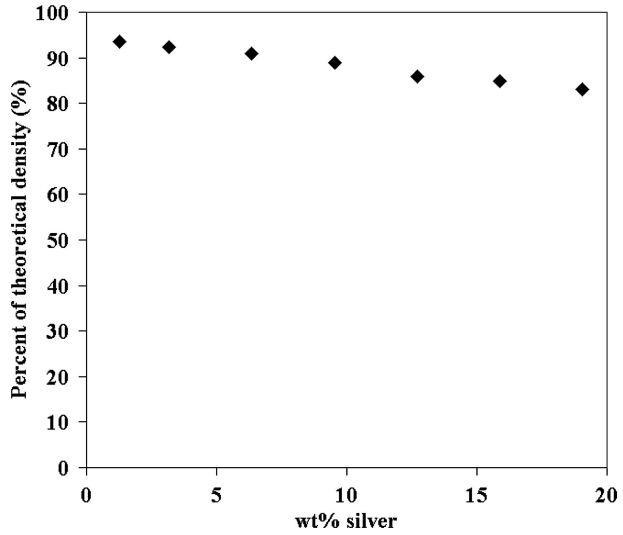

Figure 2 Variation of composite density with silver content. Error bars indicate 95% confidence limits.

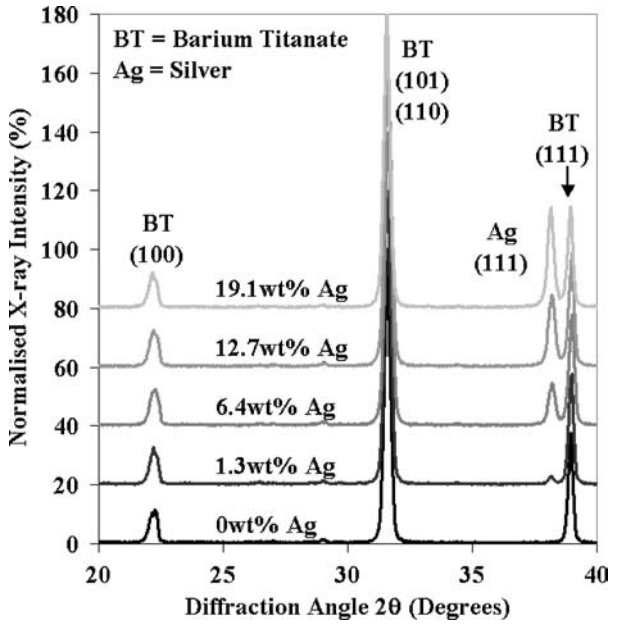

Figure 3 X-ray diffraction analysis results of various barium titanate-silver composites indicating an increasing silver peak and no unknown reaction phase peaks. Sintered at 1300°C.

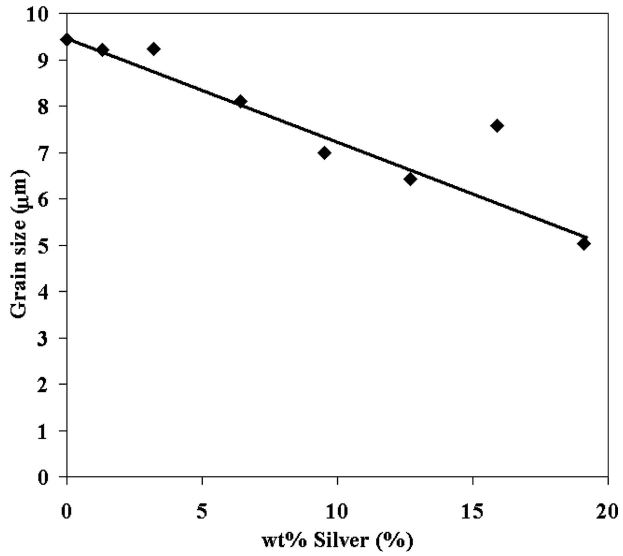

Figure 5 Decrease of barium titanate-silver grain size with the addition of silver.

XRD pattern of pure barium titanate and of composites with up to 19.1 wt.% silver. In addition to the observed increase in porosity as the silver content increases, the grain size is also modified. The grain size of the composites was determined using a scanning electron microscope (SEM), Fig. 4. Image analysis of the longest grain axis for over 200 individual grains demonstrated, as in Fig. 5, that as silver was added there was a gradual decrease from 9.4 μm (95% Confidence interval $\pm$0.65) to 5 μm (95% Confidence interval $\pm$0.28). The monolithic grain size of 9.5 μm is comparable to other studies of barium titanate [3]. Grain size has been reported to affect the relative permittivity, a maximum in permittivity occurring at a grain size of $\sim$1 μm [14–17]. It has been proposed that below a grain size of 1 μm the domain width is too large to be stable [15], while above this value microscopic internal stresses can be relieved by domain formation.

Analysis of cross sections of polished composites showed that large silver particles ($>$1 μm) were situated at grain boundaries, while those particles $<$1 μm tended to reside within the grains. It has been suggested that the

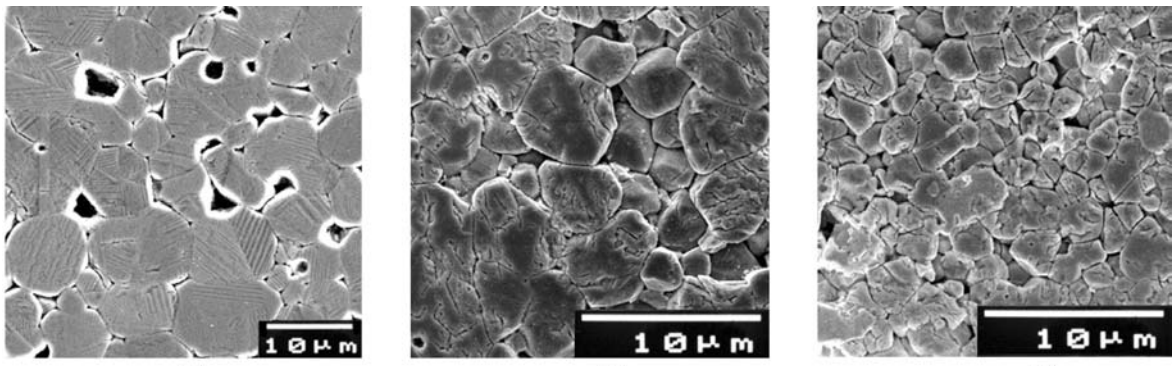

Figure 4 SEM images of (a) barium titanate, (b) $BaTiO_3$-3.2 wt.% silver composite and (c) $BaTiO_3$-19.1 wt.% silver composite.

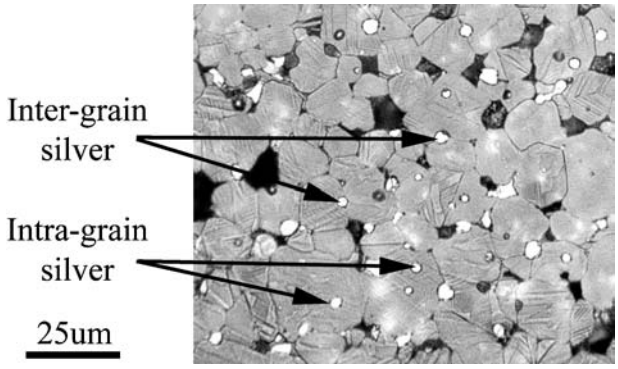

Figure 6 Silver particles within grains and at the grain boundaries in barium titanate-3.2 wt.% silver composites.

smaller particles within the grains may interact with domain wall motion at high electric fields, and influence the piezoelectric properties [18]. In addition the intergranular silver particles have potential for composite toughening by crack bridging [19]. Fig. 6 shows silver particles at grain boundaries and within grains. The average silver particle size in the sintered composites increased with increasing silver content. An average major axis length of the silver particles increased from 1.8 μm with 1.3 wt.% addition to 4.3 μm with 18 wt.% silver. Smearing of silver during sample preparation was ignored in the estimation of particle size. The increase in particle size indicates that agglomeration of the silver is taking place under the operative sintering conditions, due to its molten state. Whereas the measured grain size of the composites are lower than reported by Chen et al. [7] the silver inclusions are of comparable size. Significant numbers of abnormal grains were not observed in most samples fabricated in this study, indicating reduced chemical inhomogeneity. However, it is noted that barium titanate with 1.3 wt.% and 3.2 wt.% silver had a small number of grains about 20 μm in size.

Although no reaction phases were observed, surface silver loss due to evaporation of the molten silver at the sintering temperature was observed at the sample surface, Fig. 7. At the barium titanate sintering temperature of 1300°C the partial pressure of silver is 0.00087 atm., as calculated from the equation in [20]. This lighter-coloured surface layer has been reported earlier by Chen and Tuan [7]. The silver loss at the surface did not appear to extend into the sample core. A typical depletion layer was ~50–100 μm depth, similar to that reported by Chen and Tuan [20].

Transmission electron microscopy (TEM) revealed the near spherical geometry of the intragranular silver particles. The intergranular silver particles conformed to the grain shape. No reaction phases were observed at the barium titanate-silver interface and the ductility of the silver particles could well allow crack bridging to operate. Domain walls were observed to impinge on intragranular silver particles, as shown in Fig. 8. It is noted that the surfaces of the silver particle are coherent demonstrating an angular morphology. The change from coherent to incoherent surface correlates with the large microcrack on both sides of the silver particle. The microcrack on the left hand side of the silver particle has caused a domain wall to be offset by ~20 nm. This indicates that this contrast is not due to a dislocation, which would have a much smaller Burgers vector. It is suggested that the offset is a result of microcracking that occurred after domain formation.

The domain walls impinging on the coherent side of the silver particle are associated with a change in silver surface alignment. It is suggested that during cooling from the poling temperature the silver particle has aided in the preferential nucleation of a new domain, as the twin width is equal to that of the epitaxial face of the silver particle. The large microcrack is likely to be due to the negative hydrostatic stress generated during cooling of the

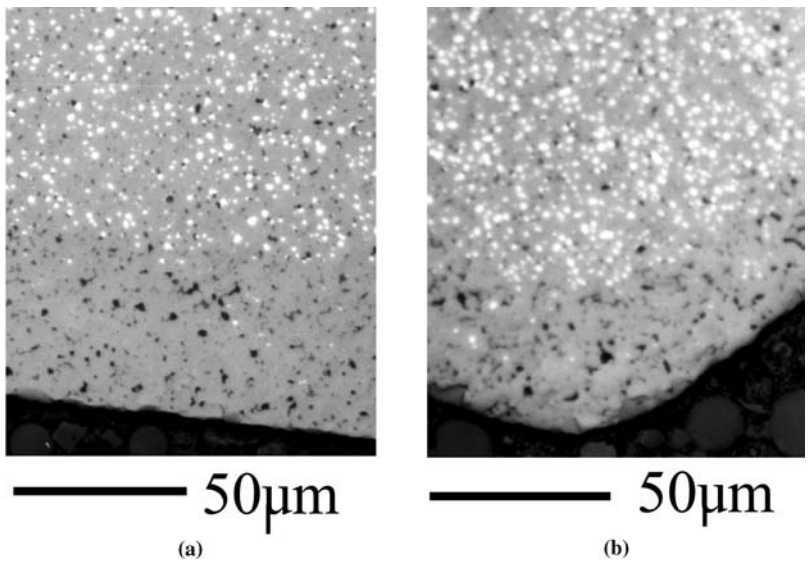

Figure 7 Silver depletion layer in barium titanate- (a) 9.3 wt.% silver and (b) 14 wt.% silver. Grey phase is barium titanate and white regions are silver particles.

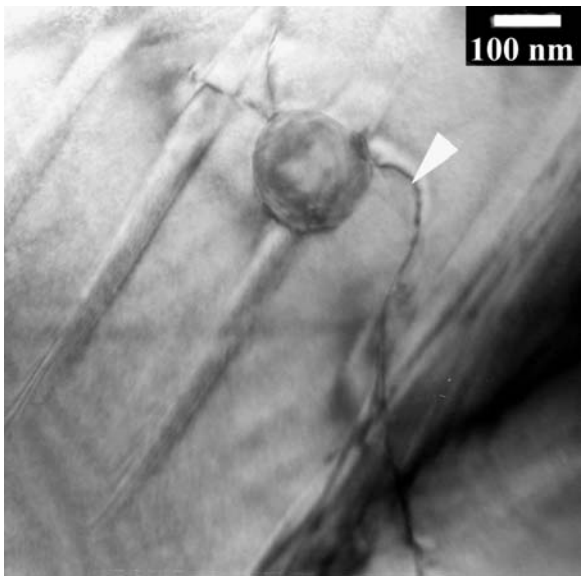

Figure 8 Observation of domain interaction with silver particles in barium titanate-3.2 wt.% silver. White arrow indicates a large microcrack.

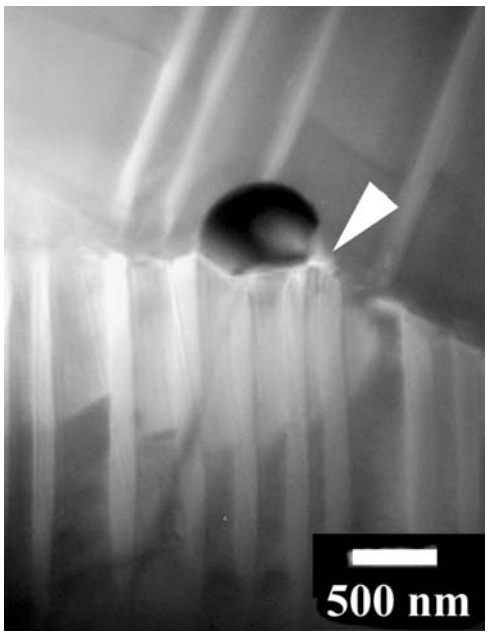

Figure 9 Micro-crack (indicated by white arrow) generation in the presence of intra-granular silver particles at the end of a twin/domain boundary.

silver particle resulting in a significant tensile component. Intergranular silver particles revealed the relief of thermal residual stress, caused by differing coefficients of thermal expansion, by the formation of micro-cracks, as shown in Fig. 9. The calculated thermal residual stress in the barium titanate-silver system is ∼1400 MPa (the relationship is given in [21] and values in [22] for a temperature change of 1300°C). Fig. 9 shows that the silver particle is at a grain boundary and has both coherent and incoherent surfaces, similar to the particle shown in Fig 8.

In the absence of an appropriate electric field it is not known whether the motion of the domains will be

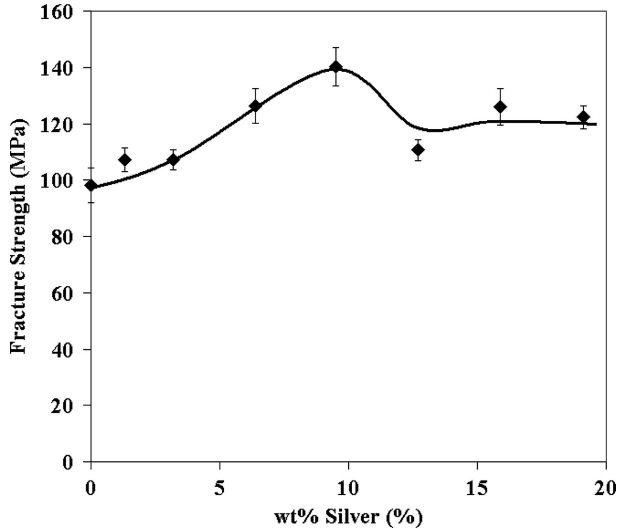

Figure 10 Variation of fracture strength with silver content. Error bars indicate 95% confidence limits.

driven, although polarisation-field measurements can provide details of the possible influences of silver particles on polarisation behaviour and are to be presented in Part II.

3.3. Mechanical testing

Typical values for pressureless sintered barium titanate were measured, with a strength of 100 MPa and a fracture toughness of ∼2 MPa.m$^{0.5}$. Incorporation of silver into barium titanate increased the strength of the composites from 100 MPa to 120 MPa with 19.1 wt.% silver addition, as shown in Fig. 10. Initially, below 10 wt.% silver, the increase in strength was more pronounced, achieving 140 MPa at 10 wt.% silver. The decrease in strength above 10 wt.% silver is believed to be caused by the increased porosity present at high silver contents. An improvement in the strength with the addition of up to 15 vol.% platinum to PZT has been reported [2]. The authors proposed that the strength increase was be due to the improvement in the fracture toughness according to Griffith's theory. Formation of thermal residual stresses was given as the reason for a plateau in strength above 15 vol.%. An intragranular fracture mode observed for the monolithic barium titanate has been reported in literature [23, 24] and is shown in Fig. 11a.

The addition of silver to barium titanate did not change the fracture mode, as shown in Fig. 11b, although samples with high silver contents were observed not to fracture completely. This is likely to be due to the presence of silver filaments bridging the fracture surfaces and examples of these filament pull-outs and cup-cone features reminiscent of ductile failure are given in Fig. 12. This mechanism would be expected to improve the fracture toughness. However, incorporation of silver did not significantly improve the fracture toughness as determined by indentation. The measured fracture toughness was

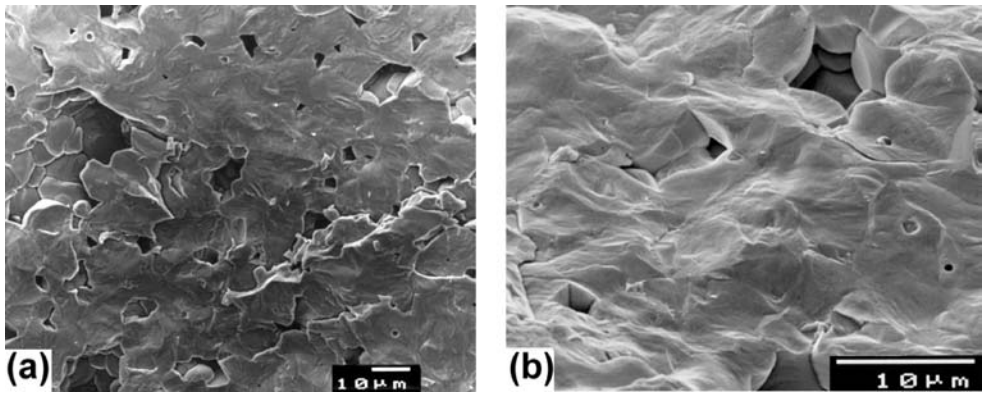

Figure 11 Intragranular fracture mode for (a) monolithic barium titanate and (b) barium titanate-3.2 wt.% silver.

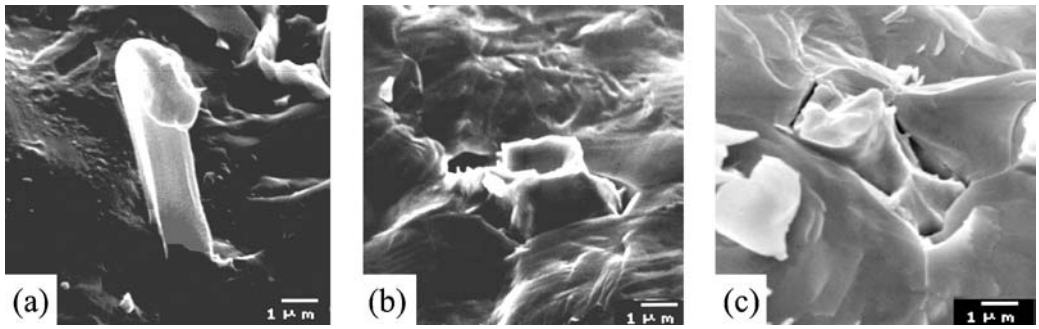

Figure 12 Barium titanate-6.4 wt.% silver indicating the ductile behaviour of the silver particles by (a) pull-out and (b) and (c) cup-cone fracture zone.

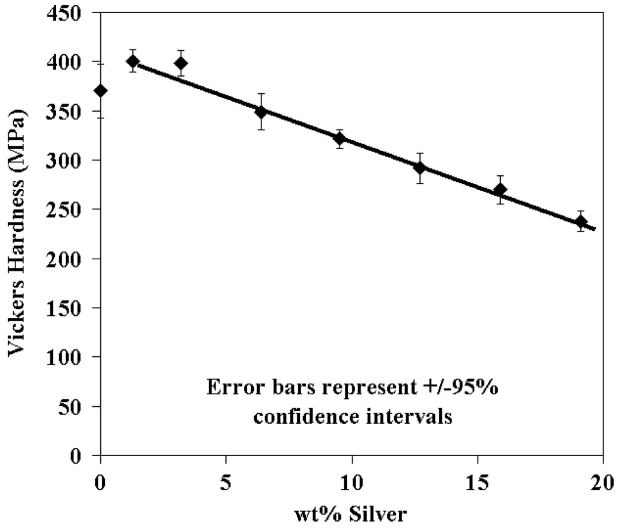

Figure 13 Variation of composite hardness with silver content. Error bars indicate 95% confidence limits.

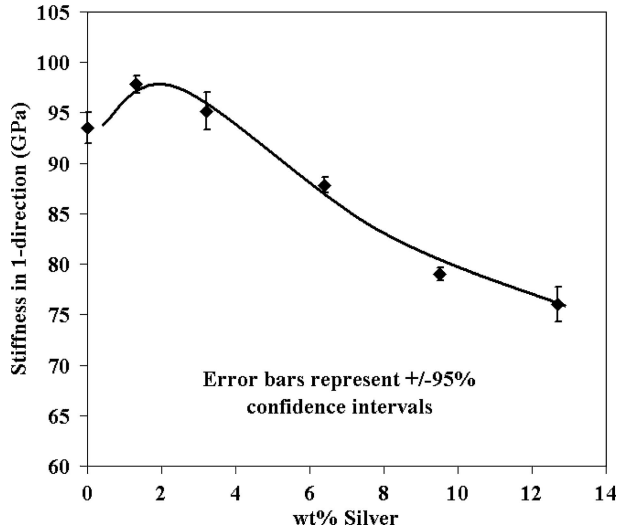

Figure 14 Variation of stiffness in the 1-direction ($1/S_{11}$) with the addition of silver to barium titanate.

$\sim$2.0 MPa.m$^{0.5}$ for monolithic barium titanate and for the composites the toughness varied between 2.0 MPa.m$^{0.5}$ and 2.3 MPa.m$^{0.5}$. The 95% confidence intervals were typically $\sim$0.15 MPa.m$^{0.5}$. Chen and Tuan reported no large increase in fracture toughness [3]. The measured fracture toughness did not improve with silver addition, suggesting an increase in the strength needs to be attributed to other mechanisms. However, determination of the facture toughness by the indentation technique would not promote crack bridging by silver particles. The cracks produced by the Vickers indent propagate along grain boundaries and the barium titanate-silver interface. This is in contrast to the cracks passing though the silver particles in tensile samples when the silver particles embedded in the barium titanate matrix can undergo ductile deformation, as shown in Fig. 12.

The hardness of monolithic barium titanate was 4 GPa; it initially increased, but reduced to 2.5 GPa with silver

additions up to 19 wt.% silver, Fig. 13, as expected with incorporation of a mechanically softer ductile phase. The silver composites showed a decrease in stiffness with silver content, Fig. 14.

4. Conclusions

Composites of barium titanate with various volume fractions of silver particle additions were successfully fabricated. No reaction occurred between the barium titanate and silver particles as determined by X-ray diffraction analysis and transmission electron microscopy. Dilatometry revealed that the addition of silver to barium titanate initiates densification earlier and produces a plateau in the shrinkage rate-temperature plot. Silver inhibits the densification of barium titanate, due to limited solubility of the sintering species in the intergranular silver that reduces the diffusion along the grain boundaries. Grain boundaries can become pinned to the large silver particles reducing the grain size. Silver particles below 1 μm in size were located within the grains and were observed using TEM to be attached to domain walls and dislocations. The size of the silver particles in the composites increased by 30% with increase in the silver content from 1.3 wt.% to approximately 18 wt.%.

The strength of barium titanate was improved with the addition of silver particles. A silver content of 10 wt.% increased the strength from 100 MPa to 140 MPa. No significant change in fracture toughness was observed with the addition of silver, suggesting that any beneficial crack bridging by the silver inclusions is minimal. The stiffness and hardness decreased with increasing silver content, attributed to the softness of the silver compared to barium titanate.

Acknowledgments

The authors would like to thank the UK Engineering and Physical Science Research Council (EPSRC) for funding this research.

References

1. K. TAJIMA, H. HWANG, M. SANDO and K. NIIHARA, *J. Am. Ceram. Soc.* **83** (2000) 651.
2. J-F. LI, K. TAKAGI, N. TERAKUBO and R. WATANABE, *Appl. Phys. Lett.* **79** (2001) 2441.
3. C. CHEN and W. TUAN, *Mat. Sci. Lett.* **18** (1999) 353.
4. D. THOMPSON and H. MANDAL, in "21st Century Ceramics" (The University Press, Cambridge, 1996) p. 225.
5. H. HWANG and K. NIIHARA, *J. Mat. Sci.* **33** (1998) 549.
6. S. PANTENY, R. STEVENS and C. BOWEN, in Proceedings of Ferroelectrics 2000 UK, 2000, edited by N. Alford and E. Yeatman (IOM Communications Ltd, London, 2000) p. 75.
7. C-Y. CHEN and W-H. TUAN, *J. Am. Ceram. Soc.* **83** (2000) 2988.
8. S-J. SHIH and W-H. TUAN, *ibid.* **87** (2004) 401.
9. R. CHEN, X. WANG, Z. GUI and L. LI, *ibid.* **86** (2003) 1022.
10. N. HALDER, A. DAS SHARMA, S. KHAN, A. SEN and H. MAITI, *Mat. Res. Bull.* **34** (1999) 545.
11. C. SAUCY, I. REANEY and A. BELL, *Brit. Ceram. Proc.* **51** (1993) 29.
12. M-H. LIM, J-F. CHOU and H-Y. LU, *J. Euro. Ceram. Soc.* **20** (2000) 517.
13. I. CLARK, F. MARQUIS and D. SINCLAIR, *ibid.* **22** (2002) 579.
14. K. GACHIGI, U. KUMAR and J. DOUGHERTY, in Proceedings of the 8th IEEE International Symposium on application of ferroelectrics, Greenville, September 1992, edited by M. Liu, A. Safari, A. Kingon and G. Haertling (ISAF'92) p. 492.
15. A. BELL and A. MOULSON, *Brit. Ceram. Soc.* **36** (1985) 57.
16. G. ARLT, D. HENNINGS and G. DE WITH, *J. Appl. Phys.* **58** (1985) 1619.
17. W. LUAN, L. GAO and J. GUO, *Ceram. Int.* **25** (1999) 727.
18. G. ARLT, *Ferroelectrics* **76** (1987) 451.
19. H. HWANG, M. YASUOKA, M. SANDO, M. TORIYAMA and K. NIIHARA, *J. Am. Ceram. Soc.* **82** (1999) 2417.
20. C-Y. CHEN and W-H. TUAN, *ibid.* **83** (2000) 1693.
21. H. HWANG, T. NAGAI, T. OHJI, M. SANDO, M. TORIYAMA and K. NIIHARA, *ibid.* **81** (1998) 709.
22. H. HWANG, T. SEKINO, K. OTA and K. NIIHARA, *J. Mat. Sci.* **31** (1996) 4617.
23. F. MESCHKE, A. KOLLECK and A. SCHNEIDER, *J. Euro. Ceram. Soc.* **17** (1997) 1143.
24. R. POHANKA, R. RICE and B. WALKER, *J. Am. Ceram. Soc.* **59** (1976) 71.

Received 7 July 2004
and accepted 13 July 2005